2012

Mountain bike wheel endurance testing and modeling

Robin C. Redfield

United States Air Force Academy, rob.redfield@usafa.edu

Cory Sutela

SRAM LLC

Redfield, Robin C. and Sutela, Cory, "Mountain bike wheel endurance testing and modeling" (2012). *U.S. Air Force Research*. 73.
http://digitalcommons.unl.edu/usafresearch/73

9th Conference of the International Sports Engineering Association (ISEA)

Mountain bike wheel endurance testing and modeling

Robin C. Redfield[a,*], Cory Sutela[b]

[a]*Department of Engineering Mechanics, United States Air Force Academy, Colorado Springs, Colorado U.S.A.*
[b]*Colorado Development Center, SRAM LLC, Colorado Springs, Colorado U.S.A.*

Abstract

Mountain bike wheels may be evaluated for durability and mode of failure using bump drum test machines that subject wheels to simulated rider loads and uneven terrain. These machines may operate at high speeds in order to accelerate failures, particularly during the design and prototype phase of wheel development. This paper describes a mathematical model of the dynamics of a wheel test drum assembly, and the validation of the model using data recorded during a wheel test. This model will subsequently be applied to better understand the key test operating parameters that must be controlled in order to produce repeatable durability data during accelerated testing.

Keywords: Mountain biking; wheels; failure testing

1. Introduction

Mountain bike (MTB) wheels are subject to a wide range of loading conditions. The most moderate inputs in the radial direction typically arise from the mass of the rider, long wavelength ground unevenness, and low amplitude surface roughness. In the lateral direction, cornering loads may also be relatively moderate in magnitude. These smaller loads are primarily absorbed by rider body motion and tire deformation. More extreme excitations include radial and lateral loads caused by high frequency or step inputs: rocks, roots, and trail discontinuities. These larger loads induce significant stress on the wheel structure; damage from this stress accumulates over the life of the wheel and leads to part failure.

MTB wheels must be designed to withstand many miles of this loading before failure. Typical failure modes include loss of lateral stability, spoke breakage, and rim or hub cracking. One method of

* Corresponding author. Tel.: 719-333-4396.
E-mail address: rob.redfield@usafa.edu.

determining wheel robustness is through hours of harsh trail testing, however this is time consuming and generally not suitable for rapid development of optimum wheel designs.

Accelerated damage accumulation is accomplished in the laboratory through cyclic loading of wheels in simulated riding conditions, which are difficult to define.

One widely accepted method of accelerating wheel failure is the so-called bump drum, a rotating drum with protrusions placed in the wheel path along the drum circumference. The drum may be rotated at varying speeds and is typically of larger diameter than the wheel in order to ensure a realistic contact surface between the drum and the tire. The protrusions, or bumps, can be shaped and spaced along the drum as desired. A test wheel, fully assembled with an inflated tire, is held in contact with the rotating drum and rotates freely as damage accumulates over hours or days. Wheels are inspected at regular intervals and may be monitored with a variety of instruments. Previous published research on wheel testing includes [1] where aerodynamics, inertial properties, stiffness, and bearing resistance are considered and [2], an investigation of spoke patterns and their effect on fatigue life. In [3], radial stiffness and spoke load distribution is examined. To the authors' knowledge, little or no research has been published concerning endurance testing on wheel test machines.

This paper presents the development of a mathematical model of the dynamics of a drum test machine, along with experimental data used to validate the model. The evolution of the model reflects the insight gained into the nature of the experimental results, as model parameters were added and adjusted to match the observed test behavior. Ultimately this model will be used to predict dynamic behavior with two objectives: to reduce the time required for reliable evaluation of prototype wheels, and to improve the consistency in time to failure observed on similar test machines in different test laboratories

2. Equipment - Bump drum test rig

Figure 1a shows a typical wheel testing assembly supported inside a safety enclosure. In this configuration a fully assembled wheel is mounted (using a standard bicycle axle) to a pivoting assembly consisting of two parallel, extruded aluminum arms. These are fixed in space at one end as shown schematically in Figure 1b. The wheel rolls on the 866 mm diameter drum below which is driven at a constant angular velocity by a 7.5 hp electric motor. The pivot assembly is adjusted so that with the wheel resting on the drum, the arms are parallel to the ground and the motion of the wheel is nearly vertical. Radial load, simulating bike and rider mass, is added using weights supported near the wheel hub axis. The pivoting assembly is raised and lowered on pneumatic actuators during wheel installation. Ten bumps of height 18 mm are evenly spaced around the circumference of the drum.

The pivot assembly is instrumented with displacement transducers and switches used for test monitoring and control. For this study, the 2D acceleration (vertical and lateral) of the bicycle hub in the plane of the wheel was recorded using a multi-axis accelerometer (Neuwghent model TAA-3000).

The rig was parameterized for subsequent modeling through measurement and testing. The schematic in Figure 1b indicates the translational and angular velocities that were considered in the model. Relevant dimensions and masses were measured from the rig. The location of the center of mass of the pivot arm and its natural frequency of rotation about the pivot were used to determine the mass moment of inertia (MMI) of the pivot assembly. The MMI of the entire moving assembly about the pivot and the effective gravitational torque acting on the assembly were calculated for use in the model. The stiffness of the wheel assembly with the tire inflated to three pressures (138, 276 and 414 kPa) was determined using fixtures simulating the drum, and then, the bump, using an instrumented hydraulic load frame. The method of [4] was followed to fit power functions to these two geometric configurations. When the tire interfaces with a bump, the tire deforms around the bump until part of the tire contacts the drum. In cases when the radial load on the wheel was sufficient to induce this contact, the two stiffnesses were added in parallel.
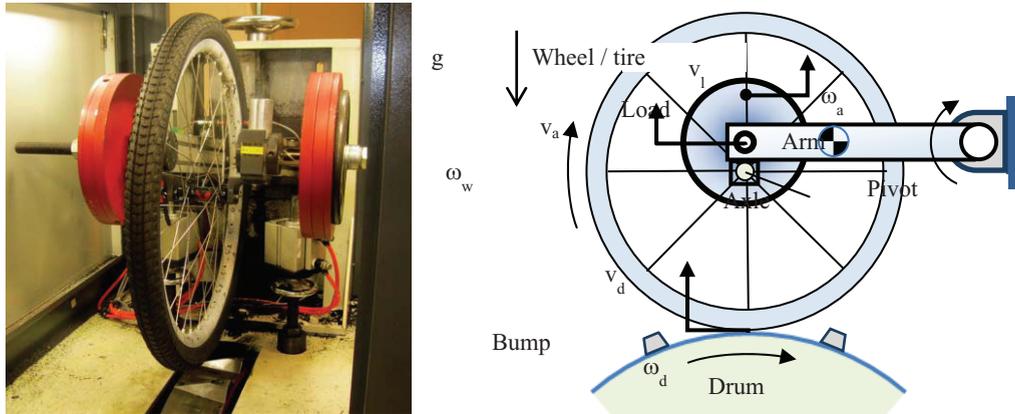
Fig. 1. (a) Bump drum test rig; (b) Bump drum, wheel, and loading schematic

Figure 2a shows the measured wheel/tire radial stiffness at a tire pressure of 276 kPa. At very low load the rubber casing of the tire is relatively compliant, but its stiffness increases rapidly as the pressurized tire system is loaded, and its constitutive behavior becomes nearly linear. The stiffness measured with the tire in contact with a bump is up to 60% less than when measured with the tire in contact with the drum. This is due to the smaller contact area between the bump and the tire.

The modeled wheel/tire radial stiffness under the same conditions is shown Figure 2b. A sigmoid function was used to model the transition from the unloaded condition to the region with linear stiffness.
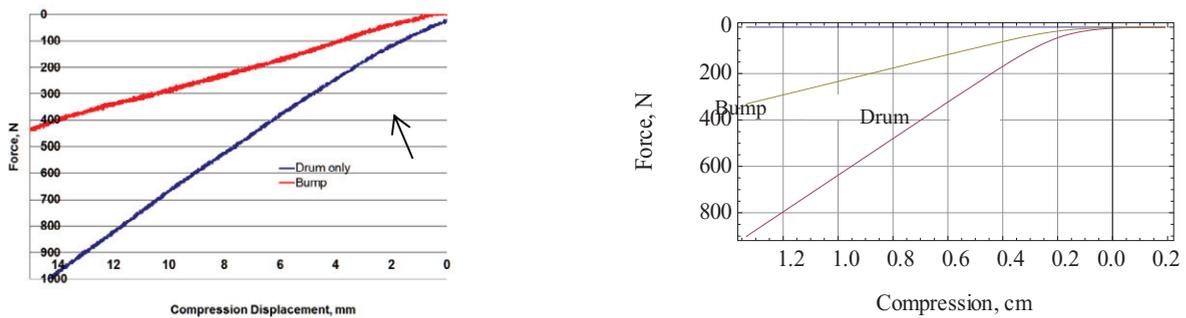

Fig. 2. (a) Measured tire load-deflection relationship; (b) Model sigmoid function for tire load-deflection relationship

3. Dynamic model of test machine

The model of the test rig with the wheel and tire incorporates the inertia of the arm, wheel, and weights, the compliance of the wheel/tire, the out-of-plane stiffness of the support for the weights, and the internal damping of the structure and pivot. The input to the model is the profile of the bump drum accounting for the spacing and profile of the bumps. A bond graph model of the test rig is shown in Figure 3a. Bond graphs are precise, pictorial representations of the significant power interactions, energy storages, and dissipations of a system. The uneven surface of the drum provides an energy input to the model. This energy is tracked through the tire and wheel, the pivot arm, and results in the dynamics observed at the pivot and weights. The support arm rotational inertia is represented by I_o, damping by b_o, and gravitational torque by τ_{mg}. The rod and weight sub-assembly are modeled with compliance and damping, k_r and b_r; weight, $m_l g$; and mass, m_l.

Figure 3b depicts the geometry of the interface between the uneven drum surface and the tire. Wheel and drum radii are r_w and r_d, bump height is h_b, and horizontal distance from bump to center is d. Depending on the vertical position of the wheel and its proximity to a bump on the drum surface, the interface between the tire and the test rig is modeled in one of three conditions: 1) the wheel is bouncing and the tire not in contact with any surface, 2) the tire is in contact with either the drum or a bump, or 3) the tire is in contact with both the drum and a bump simultaneously. At any instant, the vertical position of the wheel hub along with the angular position of the nearest bump determine the distance between the wheel center and both the drum surface and closest bump. If either of these distances are less than the tire radius, the tire is compressed, and the model determines the contact force(s) at the interface. Figure 4 describes the state of the tire compression response to bumps, relative to bump spacing. The horizontal sections of this graph showing zero bump compression represent the condition when the tire is centered between bumps, and no additional tire compression is added to account for bumps. When a bump is encountered, as much as 1.8cm of tire compression results as the tire rolls over the bump.

Fig. 3. (a) Bond graph model of test rig dynamics; (b) Bump drum – tire interface geometry

Fig. 4. Tire compression due to bumps, relative to bump location

4. Experimental data

Measured wheel-center vertical acceleration data, displayed in Figure 5 on two different time scales, illustrate various aspects of the system dynamic behavior. The data shown were recorded for a 276 kPa tire pressure and a 74 cm (29 in) diameter tire with the drum operating at a linear speed of 40 km/hr. The most obvious dynamic has a period of about 0.025 seconds, corresponding to an input frequency of 40 Hz, and represents the system response to bumps as they contact the tire at this frequency. Accelerations

in the negative direction indicate unweighting and even hopping of the tire and pivot arm. This portion of motion creates a more rounded curve on the time-acceleration graph denoting a slightly lower frequency. The positive accelerations correspond to compression of the tire and its resultant increased stiffness with drum or drum/bump contact, creating a higher frequency behavior.

A lower frequency oscillation with period ~0.2 seconds corresponds with the 5 Hz natural frequency of the weighted pivot arm on the pneumatic tire. A higher frequency oscillation is also observed in the experimental data, with a period of nearly 0.0025 seconds and could be attributed to a torsional/bending oscillation induced by the force of the loading masses, coupled through the rods and arms supporting them. In this hypothesis the resistance to this mode of oscillation would be the stiffness of the supporting rods and the torsional stiffness of the arm (Figure 1). This is allowed for in the model by the degree of freedom between the load and the arm, V_l versus V_a, in Figure 1b.
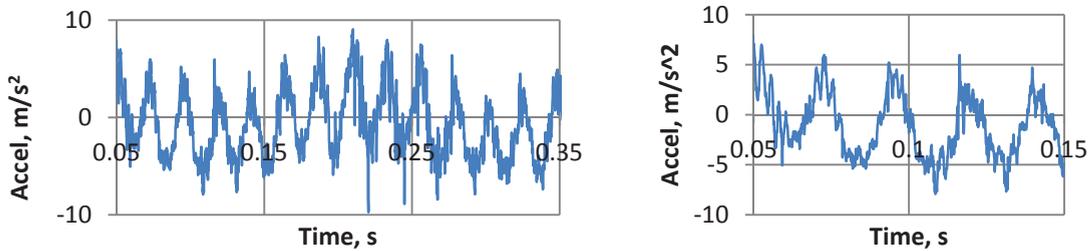

Fig. 5. (a) 0.3 seconds of acceleration data; (b) 0.1 seconds of acceleration data

5. Model results

Model results for the operational conditions above (a linear speed of 40 km/h and tire pressure 276 kPa) are shown in Figure 6. The predicted linear acceleration of the pivot arm is shown in Figure 6a. Damping ratios for the arm rotation (0.12) and the bending of the rods supporting the weights (0.04) were tuned to match the model to the experimental data. The model results are similar in nature to the experimental observations. The 5 Hz oscillation of the pivot arm supported by the pressurized air in the tire is observed with the 40 Hz bump frequency added to it. The amplitude of the accelerations caused by the bumps are similar to those in the experimental data, about +/- 5 m/s². The shape of the bump-induced acceleration curve is similar to the experimental data in that the plot is lower in curvature (thus frequency) for negative acceleration than for positive values because drum contact (versus bump only) results in a greater system stiffness. The model also predicts the higher frequency oscillations due to the bending/torsion of the rod supporting the weights. This highest frequency model output might be mistaken for noise in the experimental data.

Figure 6b shows both the position of the arm and the radial force on the tire. Both of these values are normalized with respect to their equilibrium (eq) values: equilibrium tire deflection and equilibrium tire force. The 5 Hz natural frequency of the pivot arm is illustrated in the predicted displacement. The normalized equilibrium position would be -1 but the average value of position is greater due to the repeated bump inputs. Normalized tire force is displayed on the same scale and shows the contributions from drum and bump contact. The low frequency changes in tire contact force are due to the motion of the pivot arm. The higher frequency oscillation is due to bump contact with the tire.

Figure 7 shows the same model outputs for a 10 km/hr linear velocity at the drum surface, ¼ the speed of the previous results. The amplitude of the acceleration is predicted similar to the 40 km/hr result but predicted tire forces have a greater range than the 40 km/hr case. At this speed the pivot arm motion is

affected to a relatively greater degree by bump impacts than under faster conditions. Similar behavior can be observed when a vehicle with suspension travels over a wash-board road at various speeds.
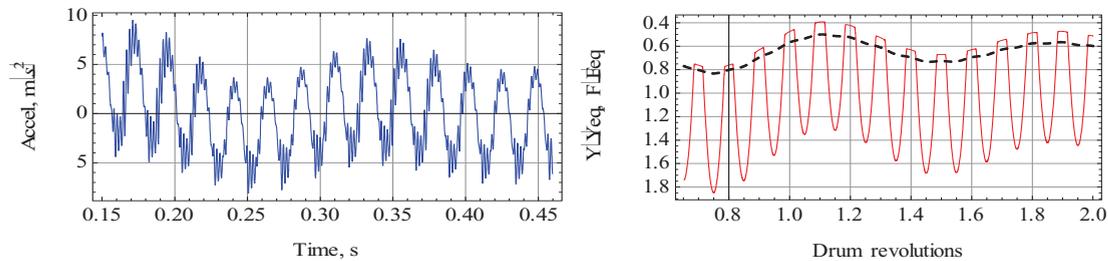

Fig. 6. (a) 40 km/hr model arm acceleration; (b) 40 km/hr normalized model arm motion (dashed) and tire force (solid)
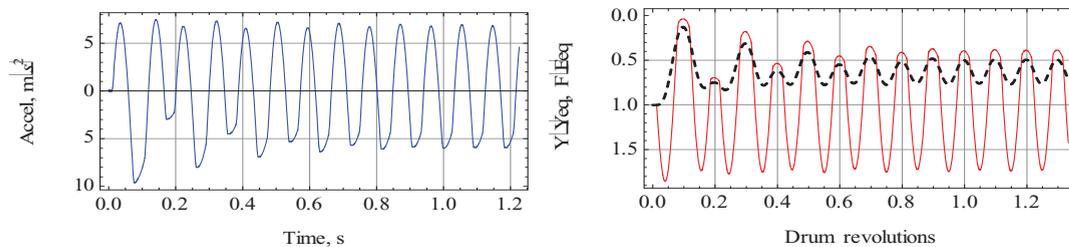

Fig. 7. (a) 10 km/hr arm acceleration; (b) normalized 10 km/hr arm motion (dashed) and tire force (solid)

6. Discussion

The goal of building a model of the bump drum test rig was to gain insight into the parameters which have a significant effect on loading on the wheel. By modeling the motions of the pivot arm, dynamic behavior that is difficult to identify experimentally can be studied and applied to reduce variability in test results. In the development of this model, insight was gained into the mechanisms that create certain features observed in the experimental data. The insight will be applied in the next step of this study, when the model is validated over a wider range of operating conditions and then used to identify the conditions that result in acceptable insensitivity to expected changes in test inputs. Ultimately this will allow accelerated testing with results that are repeatable on a variety of test machines.

Acknowledgements

References

[1] Roues Artisanales.com, 2008, "Great wheel test of 2008", http://www.rouesartisanales.com/article-15441821.html.
[2] Gavin, H. P., 1996, "Bicycle Wheel Spoke Patterns and Spoke Fatigue", ASCE Journal of Engineering Mechanics., 22 (8), 736-742.
[3] Minguez, J. M. and Vogwell, J., 2008 "An analytical model to study the radial stiffness and spoke load distribution in a modern racitng bicycle wheel", Proceedings of the Institution of Mechanical Engineers, Part C: Journal of Mechanical Engineering Science, 222 (4), pp. 563-576.
[4] Moore, D. F., Wang, E. L., and Hull, M. L., 1996, "Empirical Model for Determining the Radial Force-Deflection Characteristics of Off-Road bicycle Tyres," International Journal of Vehicle Design, 17 (4), 471-482.